Processing and Application of Ceramics 7 [1] (2013) 29–35
DOI: 10.2298/PAC1301029S

Enhanced ferroelectricity and magnetoelectricity in $0.75BaTiO_3$-$0.25BaFe_{12}O_{19}$ by spark plasma sintering

Adiraj Srinivas[1,*], Muthuvel Manivel Raja[1], Duraisamy Sivaprahasam[2], Padmanabam Saravanan[1]

[1]*Advanced Magnetics Group, Defence Metallurgical Research Laboratory, Kanchanbagh, Hyderabad - 500058, India*

[2]*International Advanced Research Centre for Powder Metallurgy and New Materials (ARCI), Balapur P.O., Hyderabad - 500005, India*

Received 4 March 2013; received in revised form 30 March 2013; accepted 31 March 2013

Abstract

Spark Plasma Sintering (SPS) technique was employed to synthesize $0.75BaTiO_3$-$0.25BaFe_{12}O_{19}$ composite. X-ray diffraction studies revealed that the composite consisted of both $BaTiO_3$ (ferroelectric phase) and $BaFe_{12}O_{19}$ (ferrimagnetic phase), respectively. The SPS treated sample showed improved ferroelectric nature when compared to conventional sintered (CS) sample. Transformation from hard to soft magnetic nature was envisaged by magnetization measurements for SPS sample. A slim hysteresis loop was recorded with a low coercivity values (390 Oe) when compared to CS sample (3900 Oe). Mossbauer spectroscopy analysis indicated that the existence of a partial amount of γ-Fe_2O_3 phase in the lattice, giving rise to soft magnetic nature. The SPS sample showed slightly higher value of magnetoelectric output of 2.95 mV/cm at 3 kOe magnetic field when compared to the CS sample (1.45 mV/cm at 3 kOe). The present investigation compares the spark plasma sintered sample with the conventional sintered sample.

Keywords: *$BaTiO_3$, multiferroics, spark plasma sintering, ferroelectric properties, magnetic properties*

I. Introduction

There has been growing interest in the study of multiferroic materials, a special class of materials in which two or three kinds of order parameters i.e., ferroelectric, ferromagnetic and ferroelastic co-exist [1]. Among multiferroics, the materials exhibiting ferromagnetic and ferroelectric ordering simultaneously are known as Magnetoelectric (ME) materials. In these materials one can expect the coupling between the magnetic and ferroelectric properties as well as their control by the application of magnetic and/or electric fields [2]. Magnetoelectric materials have great potential for applications in novel actuators and sensors with high sensitivity. However, there are very few natural magnetoelectrics that exhibit both ferromagnetic and ferroelectric behaviour at room temperature [3]. This is because the off-centre distortion responsible for ferroelectric behaviour is usually incompatible with the partially filled *d*-level which are prerequisite for ferromagnetic behaviour [4].

A strong ME effect, however, can be realized in the composites consisting of magnetostrictive and piezoelectric constituents [5]. Most studies in the past, have focused on ferrite–$(PbZr)TiO_3$/$BaTiO_3$ composites [5–9]. The mixed oxides yielded ME coefficients which are much smaller than the calculated values. This was attributed to leakage currents through the low resistivity ferrite as well as micro-cracking that resulted from mismatch of structural parameters and thermal properties between the two constituents. There have also been reports of magnetoelectric effects in layered composites such as (PZT)–$Tb_{0.3}Dy_{0.7}Fe_{1.92}$ (Terfenol-D), polyvinylidenefluoride–Terfenol-D and $Pb(Mg_{1/3}Nb_{2/3})O_3$–$PbTiO_3$–Terfenol-D [10–12].

Magnetoelectric materials are usually synthesized by different sintering routes such as solid state sintering, chemical synthesis, microwave sintering, hot pressing etc., and among all the sintering routes, one of the promising sintering route is *Spark Plasma Sin-*

* Corresponding author: tel: +91 40 24586835
fax: +91 40 24340884, e-mail: *adirajs@dmrl.drdo.in*

tering (SPS). SPS method has received much attention, because many materials can be sintered at lower temperatures within a few minutes [13,14]. In the SPS method, a powder sample is pressed in vacuum in a graphite die and heated by a pulse current. The sintering proceeds very quickly because of the spark plasma caused by the large pulse current. This method can be used in metallurgy [15], ceramics [16] and even in plastics [17].

Barium titanate, $BaTiO_3$ (denoted as BT), is a well studied ferroelectric perovskite and is considered to be a good candidate for high-performance lead-free piezoelectric applications [18]. At high temperatures $BaTiO_3$ adopts paraelectric cubic phase where the large barium ions are surrounded by 12 nearest neighbour oxygen's and each titanium ion has six oxygen ions in octahedral coordination.

Barium hexaferrite, with its chemical formula $BaFe_{12}O_{19}$ (denoted as BF), is the best-known representative of the hexaferrite family. BF is one of the most important hard magnetic materials, widely used in permanent magnets, magnetic recording media, and microwave applications, due to its fairly large magnetocrystalline anisotropy, high Curie temperature, relatively large magnetization, as well as excellent chemical stability and corrosion resistance [19]. BF crystallizes in a hexagonal structure with 64 ions per unit cell on 11 different symmetry sites. The 24 Fe^{3+} atoms are distributed over five distinct sites: three octahedral sites (12k, 2a, and 4f2), one tetrahedral site (4f1), and one bipyramidal site (2b). Its crystal structure is the so-called magnetoplumbite structure, which can be described as a stacking sequence of the basic blocks S and R [20].

In our earlier communication, we have reported the magnetoelectric coupling in $BaTiO_3$–$BaFe_{12}O_{19}$ composite system (containing 75 wt.% $BaTiO_3$ and 25 wt.% $BaFe_{12}O_{19}$, with notation 0.75BT-0.25BF) at room temperature [21]. This conventionally sintered 0.75BT-0.25BF composite showed a magnetoelectric output of 1.45 mV/cm at 6 kOe. The aim of the present investigation is to compare the conventionally sintered sample with the SPS sample and correlate the multiferroic–magnetoelectric properties.

II. Experimental

A solid state double sintering method was employed to synthesize $BaTiO_3$–$BaFe_{12}O_{19}$ compositions (containing 75 wt.% $BaTiO_3$ and 25 wt.% $BaFe_{12}O_{19}$) from stoichiometric amounts of $BaTiO_3$ and $BaFe_{12}O_{19}$ powders (Sigma Aldrich with 99.9 % purity). The powders were weighed and ground together thoroughly and cold pressed into pellets. The pellets were pre-sintered at 900 °C for 2 hours, reground to powder, re-pressed into pellets and sintered at 1250 °C for 2 hours. Sintered discs were re-ground to powder form for X-ray diffraction in a Philips diffractometer at a 2*q* scan rate of 0.2 degree per minute and at 0.02 degree steps with Cu-K_α incident radiation. The surface morphology and distribution of grains were carried out using LEO440i scanning electron microscope.

Spark plasma sintering was carried out using the model Dr. Sinter 1050 (Sumitomo Coal mining Co. Ltd., Japan). The calcined powder was poured in a cylindrical graphite die of 12 mm diameter, sintered in partial vacuum (6 Pa) for 10 min under a uniaxial pressure of 50 MPa applied throughout the sintering cycle. The sintering temperature was set at 900 °C and the heating rate was kept constant at 100 °C/min. At the end of the soaking time the power and pressure were switched off and the samples were naturally cooled inside the chamber. The SPS sintered sample was annealed at 600 °C for 1 hour for maintaining oxygen stoichiometry.

The sintered discs were polished and coated with silver paste and annealed at 600 °C for 15 minutes to obtain a good electrical contact for ferroelectric measurements at room temperature in a ferroelectric hysteresis loop tracer up to a maximum applied electric field of 25 kV/cm. The maximum polarization (P_{max}) was determined from the hysteresis plots. Prior to the measurement, the samples were poled electrically using a high electric field setup. Magnetization measurements were performed in DMS vibrating sample magnetometer at room temperature, up to a magnetic field of 20 kOe. The coercivity, the magnetic moment and the remanence values were recorded at room temperature. Mossbauer spectra were recorded using FAST comtec (Germany) spectrometer at room temperature in transmission geometry with a 25 mCi ^{57}Co source in Rhodium matrix. Prior to the experiments, the spectrometer was calibrated using a standard α-Fe foil of thickness 25 μm. The Mossbauer spectra of each powder sample were recorded for duration of about 5 days with total background counts up to 8–10 × 10^5. The Mossbauer spectra were fitted with the PCMOS – II least-square fit program [24]. Magnetoelectric measurements were carried out as discussed in our earlier reports [21]. The samples were poled electrically prior to the measurements and then placed in a magnetic field and the obtained ME voltage was recorded up to a field of 5 kOe.

III. Results and discussion

X-ray diffraction patterns of $BaTiO_3$, 0.75BT-0.25BF conventionally sintered sample, SPS treated sample and $BaFe_{12}O_{19}$ are shown in Fig. 1. All the peaks could be indexed as the BT (ferroelectric) and the BF (ferrimagnetic) phases respectively. Interestingly, no difference is noted in the peak positions for the conventionally sintered (CS) and spar plasma sintered (SPS) samples, except some change in the peak intensities. It indicates that the phase formation is achieved by SPS at lower temperature and in short-

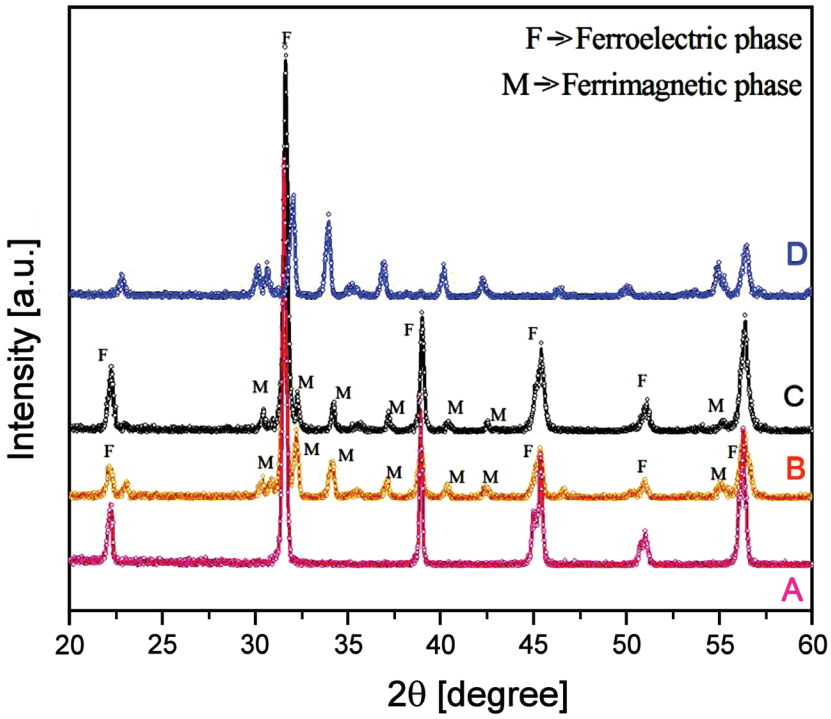

Figure 1. X ray diffraction patterns for: a) $BaTiO_3$, b) conventionally sintered 0.75BT-0.25BF, c) SPS treated 0.75BT–0.25BF and d) $BaFe_{12}O_{19}$

er sintering intervals. The structure and composition remains the same for both the phases, as there are no peak shifts even after the SPS treatment and annealing. Similar kind of results was reported in Multiferroic compounds in PZT + NiZn ferrite system and also for BF systems respectively [22,23].

Figure 2 shows the SEM images of the CS and SPS treated sample of 0.75BT-0.25BF. It is observed that the grains are distributed homogenously all over the sample for SPS treated sample. When compared to the CS sample, the SPS sample grains are formed in more compacted manner. Moreover, the hexagonal patterned grains which are significant for BF phase is evidenced in the CS treated sample, whereas, in the SPS treated sample, all BT and BF grains are nurtured giving rise to flakes/platelets kind. The reason may be due to the rapid heating rate (100 °C/min) and cooling rates (50 °C/min) during the SPS sintering. Another interesting observation arising from the Fig. 2 is that the SPS disks were nearly free of pores, with only a few pores

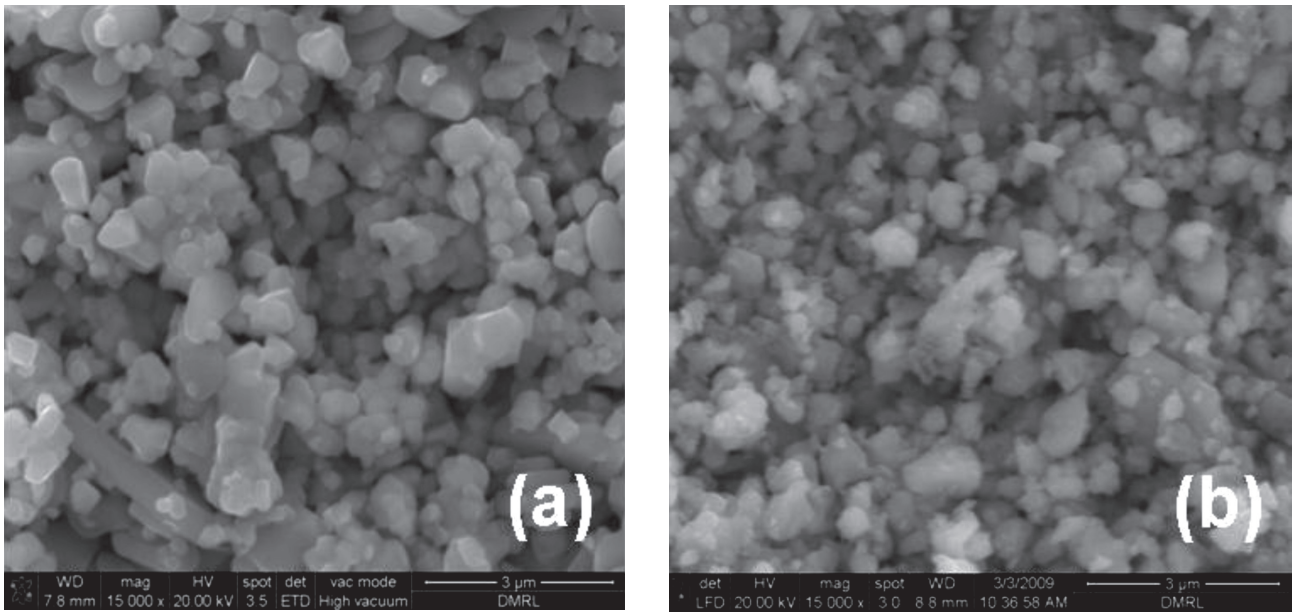

Figure 2. SEM pictures for: a) conventionally sintered 0.75BT-0.25BF and b) SPS treated 0.75BT-0.25BF samples

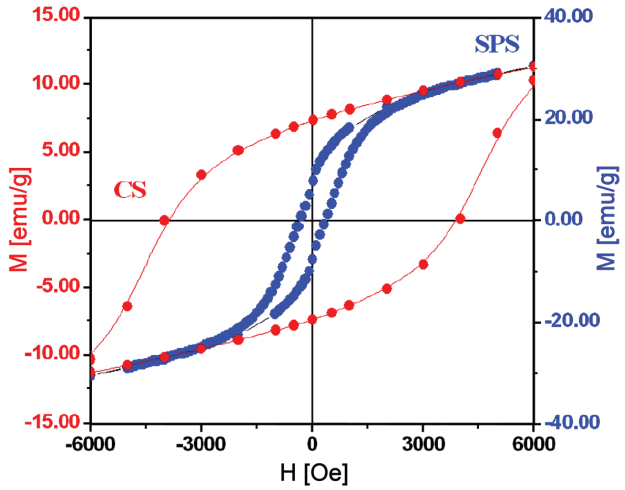

Figure 3. Magnetization versus magnetic field plots for: a) conventionally sintered 0.75BT-0.25BF and b) SPS treated 0.75BT-0.25BF

located within grains (intragranular pores). The rapid grain boundary movement caused by the superfast sintering process of SPS could explain the above finding. This result indicates that a short holding time period is an essential factor to obtain 0.75BT-0.25BF composite with uniform and fine grains by the SPS process. Similar phenomena have been reported earlier for (NiZn) Fe_2O_4 [25–27].

Figure 3 shows the magnetic hysteresis loops for the CS and SPS sintered samples at room temperature. The saturation magnetization (M_s) and coercivity (H_c) of the SPS and CS samples are enumerated in Table 1. The SPS sample showed a high saturation magnetization value (38 emu/g), when compared to CS sample (15 emu/g). Since the two samples have the same composition, the possible cause could be a difference

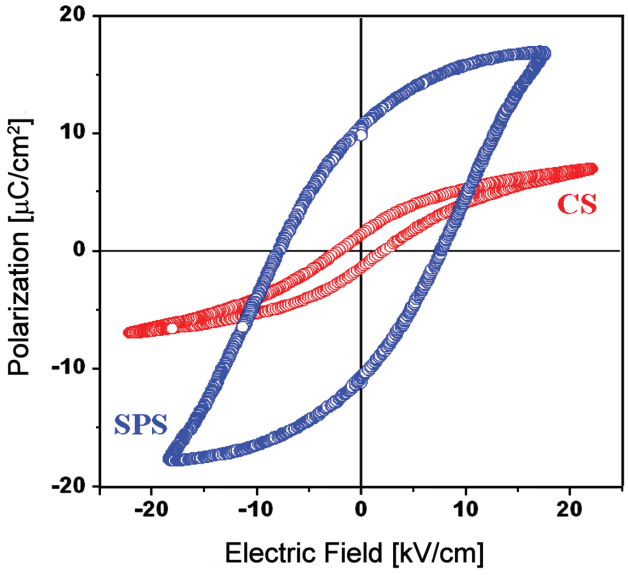

Figure 4. Polarization versus magnetic field plots for: a) conventionally sintered 0.75BT-0.25BF and b) SPS treated 0.75BT-0.25BF

in microstructure [28]. On the other hand, the SPS sample showed a very low coercivity value of 390 Oe when compared to 3900 Oe for CS treated sample. It shows that SPS treatment has a favourable effect on obtaining the soft magnetic material. It is well known that coercivity decreases with increasing density [29]. Such a decrease in samples coercivities can be attributed to the secondary crystallization which induced higher anisotropy constant and intragranular pores inhibiting the motion of domain walls [30].

Figure 4 shows the ferroelectric hysteresis loops for the CS and SPS sintered composite. The maximum polarization attained for the CS sample is 6.9 μC/cm^2 at 22 kV/cm and for the SPS sample it is 16.89 μC/cm^2 at 17.5 kV/cm. The CS sample showed a slim hysteresis loop whereas the SPS treated sample showed a broad hysteresis loop. Table 1 gives the maximum polarization, remanent polarization and coercivity values for the CS and SPS samples. All the ferroelectric properties viz maximum polarization, remanance and coercivity are higher for the SPS samples as compared to the CS sample. The possible reasons for low values for the CS sample may be due to the piezoelectric phase which is susceptible to electrical shunting and the loss of piezoelectrically generated charges due to low resistivity for hexaferrite and also due to possible presence of Fe^{2+} in the ferrite phase which could further enhance the leakage current through the sample. For the SPS sample, the density and the resistivity is much higher than for the CS sample giving a better hysteresis and ferroelectric properties for SPS sample.

Figure 5 shows the Mossbauer spectra for 0.75BT-0.25BF sample (CS), 0.75BT-0.25BF (SPS) and BF (SPS) samples. In order to understand the effect of SPS process, the Mossbauer spectra of three samples are shown. The barium hexaferrite has five crystallographically in-equivalent Fe-sites and the Mossbauer spectra were analysed with five different sextets corresponding to the five Fe-sites. The Mossbauer parameters obtained from the fitting match well with the reported values in the literature [31]. However, the Mossbauer spectra of the SPS treated samples were fitted with two or more sextets in addition to five sextets corresponding to barium-hexaferrite. The additional two sextets were necessary to obtain a satisfactory fitting and the hyperfine field values of these sextets are 490 and 500 kOe, respectively. These sextets are attributed to the presence of γ-Fe_2O_3 phase as the field values match well with the field values for this compound. The Mossbauer study indicates that the high temperature metastable γ-Fe_2O_3 phase might have formed during SPS. The Mossbauer data for the samples is presented in Table 2.

The presence of Fe^{3+} and Fe^{2+} ions has rendered piezomagnetic materials dipolar in nature. Since in piezomagnetic materials, the rotational displacement of

Table 1. Data on 0.75BT-0.25 BF composite sintered by conventional and spark plasma sintering routes

Sintering technique / parameters	P_{max} [mC/cm²]	E_c [kV/cm]	P_r [mC/cm²]	M_s [emu/g]	M_r [emu/g]	H_C [Oe]	ME output [mV/cm]
CS	6.9 (at 22 kV/cm)	2.15	1.43	15	7.5	3900	1.45 (at 3 kOe)
SPS	16.9 (at 17.5 kV/cm)	7.9	10.76	38	10	390	2.95 (at 3 kOe)

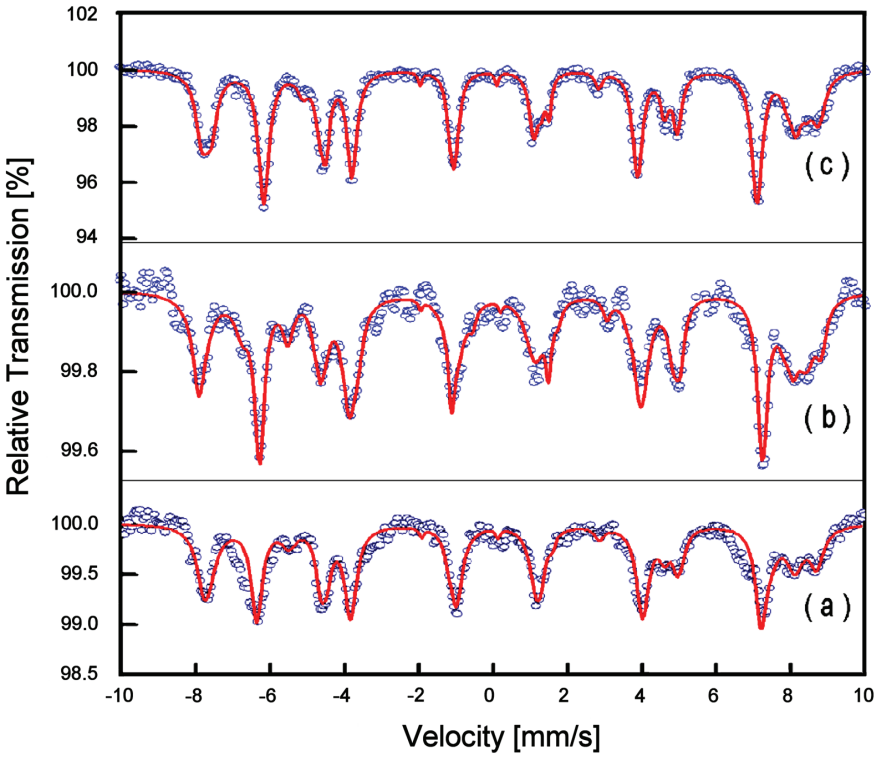

Figure 5.Mossbauer spectroscopy for: a) conventionally sintered 0.75BT-0.25BF, b) SPS treated 0.75BT-0.25BF and c) SPS treated BF

Table. 2. Mossbauer fitting parameters such as hyperfine magnetic field (B_{hf}), quadrupole splitting (*Q.S.*) and isomer shift (*I.S.*), line width (*WV*) and relative intensities (*INT*) for $BaFe_{12}O_{19}$, 0.75BT-0.25 BF (CS) and 0.75BT-0.25 BF (SPS)

Sample	Subspectra	Hyperfine parameters			*WV* [mm/s]	*INT* [%]
		B_{hf}[kOe]	*Q.S.* [mm/s]	*I.S.* [mm/s]		
$BaFe_{12}O_{19}$ (SPS)	12k	414	0.43	0.26	0.34	50
	4f1	487	0.21	0.16	0.31	17
	4f2	512	0.29	0.34	0.40	17
	2a	506	0.05	0.23	0.33	8
	2b	404	2.31	0.25	0.42	8
0.75BT-0.25BF (CS)	12k	412	0.44	0.26	0.34	50
	4f1	487	0.22	0.16	0.33	17
	4f2	516	0.34	0.33	0.40	17
	2a	505	0.01	0.26	0.34	8
	2b	403	2.24	0.24	0.43	8
0.75BT-0.25BF (SPS)	12k	411	0.42	0.26	0.34	50
	4f1	488	0.23	0.17	0.35	17
	4f2	513	0.31	0.33	0.41	17
	2a	506	0.05	0.26	0.32	8
	2b	404	2.33	0.24	0.35	8

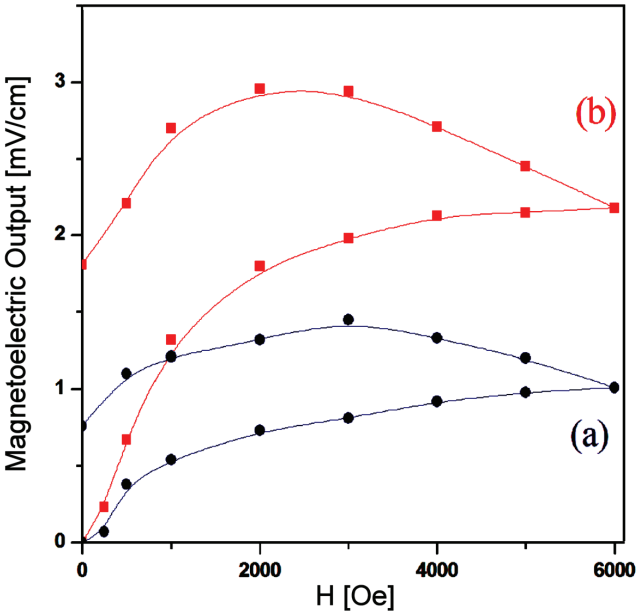

Figure 5. Magnetoelectric output for: a) conventionally sintered 0.75BT-0.25BF and b) SPS treated 0.75BT-0.25BF

$Fe^{3+} \leftrightarrow Fe^{2+}$ dipoles results in orientational polarization that may be visualized as exchange of electrons between the ions, the dipoles align themselves with the alternating field. When magnetic field is applied to the sample, the magnetoelectric output tends to increase with applied magnetic field and on decreasing the magnetic field, the output slightly increase and then decreases with a half butterfly loops indicating the strains produced during the magnetic field are not linear and a kind of relaxation (phenomenon) is taking place, giving rise to non-linearity in the system. Further studies are needed to understand the relaxation nature of the SPS treated sample.

The magnetoelectric effect is the product property of magnetostrictive and piezoelectric constituents of the composites. The ME coefficient depends on the mechanical coupling, resistivity, mole fraction of the constituent phases and importantly on sintering technique. The magnetic field dependent variations in the ME voltage is presented in Fig. 6. Table 1 gives the magnetoelectric output values of the CS and SPS treated samples at different fields. The ME output increases linearly with applied magnetic field up to a field of 5 kOe and shows a value of 2.95 mV/cm at 3 kOe when the field is reversed. The rise in output is attributed to the enhancements in elastic interactions between the piezoelectric and magnetostrictive phases. The magnetization and associated strain produce a constant electric field in the piezoelectric phase beyond the saturation limit. The possible reason for the attaining higher ME values for the SPS sample could be due to the enhancement of hyperfine fields at 12k and 2b sites as strengthening in the Fe^{3+}–O–Fe^{3+} super-exchange interaction giving higher value of magnetoelectric output. After ME output reaches to a maximum, the decrease in ME can be caused by two effects such as magnetic dilution with changing of the Fe^{3+} (high spin) valence state to Fe^{2+} (low spin) state on 2a site by substitution of the Ba^{2+} site ions and existence of spin canting which is promoting the reduction of super-exchange fields [32]. The Fe^{3+}–O–Fe^{3+} super-exchange interaction is disrupted and weakened by Fe^{2+} ions and canted spins, which could be produced by resulting in lower coercivity and magnetization for SPS treated samples [32,33].

IV. Conclusions

The SPS treated composite have showed enhanced ferroelectric properties when compared to the conventional sintered composites. The hard magnetic phase of the composite has transformed into soft phase by SPS methodology. In addition to these, the magnetoelectric output has shown high values at low fields when compared to conventional sintering. From these results, one can conclude that the SPS is favourable technique for improvement of the multiferroic and magnetoelectric properties in composites.

Acknowledgments: The authors are grateful to Shekhirev Mikhail for the SEM and TEM imaging. The authors thank Defence Research and Development Organization (DRDO), India, for the financial support to carry out this work. We express our sincere thanks to the Director, DMRL - Dr. G. Malakondaiah for his keen interest in multiferroic magnetoelectric materials.

References

1. H. Schmid, "Multi-ferroic magnetoelectrics", *Ferroelectrics*, **62** (1994) 317–338.
2. H. Schmid, "On the possibility of ferromagnetic, antiferromagnetic, ferroelectric, and ferroelastic domain reorientations in magnetic and electric fields", *Ferroelectrics*, **221** (1999) 9–17.
3. J. Wang, J.B. Neaton, H. Zheng, V. Nagarajan, S.B. Ogale, B. Liu, D. Viehland, V. Vaithyanathan, D. G. Schlom, U.V. Waghmare, N.A. Spaldin, K.M. Rade, M. Wuttig, R. Ramesh, "Epitaxial $BiFeO_3$ multiferroic thin film heterostructures", *Science*, **299** (2003) 1719–1722.
4. N.A.Hill, "Why are there so few magnetic ferroelectrics?", *J. Phys. Chem. B*, **104** (2000) 6694–6709.
5. J. Van Suchtelen, "Product properties: A new application of composite materials", *Philips Res. Rep.*, **27** (1972) 28–37.
6. J. Van Den Boomgaard, D.R. Terrell, R.A.J. Born, "An in situ grown eutectic magnetoelectric composite material", *J. Mater. Sci.*, **9** (1974) 1705–1709.
7. J. Van Den Boomgaard, A.M.J.G. Van Run, J. Van Suchtelen, "Piezoelectric-piezomagnetic composites with magnetoelectric effect", *Ferroelectrics*, **14** (1976) 727–728.

8. J. Van Den Boomgaard, A.M.J.G. Van Run, J. Van Suchetelen, **"**Magnetoelectricity in piezoelectric-magnetostrictive composites", *Ferroelectrics*, **10** (1976) 295–298.
9. G. Srinivasan, E.T. Rasmussen, J. Gallegos, R. Srinivasan, Y.I. Bokhan, V.M. Laletin, "Magnetoelectric bilayer and multilayer structures of magnetostrictive and piezoelectric oxides", *Phys. Rev. B*, **64** (2001) 214408.
10. J. Ryu, A.V. Carazo, K. Uchino, H.-E. Kim, "Magnetoelectric properties in piezoelectric and magnetostrictive laminate composites", *Jpn. J. Appl. Phys.*, **4**0 (2001) 4948–4951.
11. K. Mori, M. Wuttig, "Magnetoelectric coupling in Terfenol-D/polyvinylidenedifluoride composites", *Appl. Phys. Lett.*, **81** (2002) 100.
12. S. Dong, J.-F. Li, D. Viehland, "Ultrahigh magnetic field sensitivity in laminates of TERFENOL-D and $Pb(Mg_{1/3}Nb_{2/3})O_3$–$PbTiO_3$ crystals", *Appl. Phys. Lett*., **83** (2003) 2265.
13. J.R. Groza, A. Zavaliangos, "Sintering activation by external electrical field", *Mater. Sci. Eng. A*, **287** (2000) 171–177.
14. S.W. Wang, L.D. Chen, Y.S. Kang, M. Niino, T. Hirai, "Effect of plasma activated sintering (PAS) parameters on densification of copper powder", *Mater. Res. Bull*., **35** (2000) 619–628.
15. X. Li, A. Chiba, M. Sato, S. Takashash, "Strength and superconductivity of Nb_3Al prepared by spark plasma sintering", *J. Alloys Comp*., **336** (2002) 232–236.
16. Z. Shen, Z. Zhao, H. Peng, M. Nygren, "Formation of tough interlocking microstructures in silicon nitride ceramics by dynamic ripening", *Nature*, **417** (2002) 266–269.
17. M. Omori, "Sintering, consolidation, reaction and crystal growth by the spark plasma system (SPS)", *Mater. Sci. Eng. A*, **287** (2000) 183–188.
18. S.-E. Park, S. Wada, L. E. Cross, T. R. Shrout, "Crystallographically engineered $BaTiO_3$ single crystals for high-performance piezoelectrics", *J. Appl. Phys.*, **86** (1999) 2746.
19. M. Imanura, Y. Ito, M. Fujiki, T. Hasegawa, H. Kubaota, T. Fujiwara, "Barium ferrite perpendicular pecording flexible disk drive", *IEEE Trans. Magn*. **22** (1986) 1185–1187.
20. J. Smit, H.P.J. Wijn, p. 147 in *Ferrites*. Wiley, New York, 1957.
21. A. Srinivas, R. Gopalan, V. Chandrasekaran, "Room temperature multiferroism and magnetoelectric coupling in $BaTiO_3$-$BaFe_{12}O_{19}$ system", *Solid State Commun*., **149** (2009) 367–370.
22. Q.H. Jiang, Z.J. Shen, J.P. Zhou, Z. Shi, Ce-Wen Nan, "Magnetoelectric composites of nickel ferrite and lead zirconnate titanate prepared by spark plasma sintering"**,** *J. Eur. Ceram. Soc*., **27** (2007) 279–284.
23. R. Mazumder, D. Chakravarty, Dipten Bhattacharya, A. Sen, "Spark plasma sintering of $BiFeO_3$", *Mater. Res. Bull*., **44** (2009) 555–559.
24. T.E. Cranshaw, "The deduction of the best values of the parameters from Mossbauer spectra", *J. Phys. E*, **7** (1974) 122.
25. Z. Shen, M. Nygren, "Implications of kinetically promoted formation of metastable α-sialon phases", *J. Eur. Ceram. Soc*., **21** (2001) 611–615.
26. L. Gao, J.S. Hong, H. Miyamoto, "Bending strength and microstructure of Al_2O_3 ceramics densified by spark plasma sintering", *J. Eur. Ceram. Soc*., **20** (2000) 2149–2152.
27. T. Takeuchi, M. Tabuchi, H. Kageyama, "Preparation of dense $BaTiO_3$ ceramics with submicrometer grains by spark plasma sintering", *J. Am. Ceram. Soc*., **82** [4] (1999) 939–943.
28. M.A. Willard, Y. Nakamura, D.E. Laughlin, "Magnetic properties of ordered and disordered spinel-phase ferrimagnets", *J. Am. Ceram. Soc*., **82** [12] (1999) 3342–3346.
29. W.D. Kingery, H.K. Bowen, D.R. Uhlmann, *Introduction to Ceramics*, John Wiley & Sons, New York, 1976.
30. W.S. Kim, S.-J. Yoon, K.-Y. Kim, "Effects of sintering conditions of sintered Ni-Zn ferrites on properties of electromagnetic wave absorber"**,** *Mater. Lett*., **19** (1994) 149–155.
31. P. Sharma, R.A. Rocha, S.N. de Medeiros, A. Paesano Jr., "Structural and magnetic studies on barium hexaferrites prepared by mechanical alloying and conventional route", *J. Alloys Comp*., **443** (2007) 37–42.
32. X. Liu, W. Zhong, S. Yang, Z. Yu, B. Gu, Y. Du, "Structure and magnetic properties of La^{3+}-substituted strontium hexaferrite particles prepared by sol-gel method", *Phys. Status Solidi A*, **193** (2002) 314–319.
33. X. Liu, W. Zhong, S. Yang, Z. Yu, B. Gu, Y. Du, "Influences of La^{3+} substitution on the structure and magnetic properties of M-type strontium ferrites", *J. Magn. Magn. Mater*., **238** (2002) 207–214.